BBA - Molecular Basis of Disease 1870 (2024) 167448

Contents lists available at ScienceDirect

BBA - Molecular Basis of Disease

journal homepage: www.elsevier.com/locate/bbadis

SLFN11 and ATR as targets for overcoming cisplatin resistance in ovarian cancer cells

Philipp König [a], Julia Maria Eichhorn [a], Eloy Suparman [a], Nico Bückreiß [a], Jindrich Cinatl [b,c], Martin Michaelis [c,d], Gerd Bendas [a,*]

[a] Department of Pharmacy, University Bonn, 53121 Bonn, Germany
[b] Institute of Medical Virology, University Hospital Frankfurt, Goethe University, 60596 Frankfurt am Main, Germany
[c] Interdisciplinary Laboratory for Paediatric Tumour and Virus Research, Dr. Petra Joh Research Institute, 60528 Frankfurt am Main, Germany
[d] School of Biosciences, Division of Natural Sciences, University of Kent, Canterbury, Kent CT2 7NJ, UK

ARTICLE INFO

Keywords:
Chemoresistance
DNA repair
Epigenetics
Novel therapeutics
Ovarian cancer

ABSTRACT

The levels and activities of the DNA/RNA helicase schlafen11 (SLFN11) and the serine/threonine-protein kinase ataxia telangiectasia and Rad3-related protein (ATR) may determine cancer cell sensitivity to DNA damaging agents, including platinum drugs. Here, we studied the roles of SLFN11 and ATR in cisplatin resistance of ovarian cancer using cell lines displaying acquired or intrinsic cisplatin resistance. W1CR, the cisplatin-resistant subline of W1 ovarian cancer cells, displayed reduced SLFN11 levels. HDAC inhibition using entinostat returned an epigenetic downregulation of SLFN11 in W1CR cells, caused SLFN11 re-expression and re-sensitized these cells to cisplatin. Moreover, entinostat also sensitized intrinsically resistant EFO21 ovarian cancer cells to cisplatin by upregulating SLFN11. However, SLFN11 was not involved in cisplatin resistance in all other cell models. Thus, SLFN11 expression is not a general cisplatin resistance marker in ovarian cancer. In contrast, inhibition of the DNA damage repair master regulator ATR using sub-toxic concentrations of elimusertib sensitized parental cell lines as well as intrinsically resistant EFO21 cells to cisplatin, and fully reversed acquired cisplatin resistance in cisplatin-adapted sublines W1CR, A2780cis, and Kuramochi^{r}CDDP^{2000}. Mechanisms underlying ATR-mediated cisplatin resistance differed between the cell lines and included CHK1/WEE1 signaling and induction of homologous recombination. In conclusion, SLFN11 and ATR are involved in ovarian cancer cisplatin resistance. Although our data identify ATR as key target for tackling cisplatin resistance in ovarian cancer, future studies are needed to identify biomarkers that indicate, which individual ovarian cancers benefit from SLFN11 re-activation and/or ATR inhibition.

1. Introduction

Ovarian cancer is associated with the highest mortality rate of all gynecological cancers [1]. Approximately half of ovarian cancer patients die within five years after the diagnosis [2]. Standard therapies for ovarian cancer consist of surgery followed by chemotherapy with platinum-based drugs and paclitaxel [3]. While patients usually respond well to first-line therapy, tumor recurrence and the formation of chemoresistance often occur. Common resistance mechanisms include reduced cellular drug uptake, increased drug efflux, enhanced DNA repair, and epigenetic downregulation of pro-apoptotic proteins [4]. Notably, the epigenetic downregulation of tumor suppressors is a novel and comparatively little investigated resistance mechanism and therapeutic target. One promising example is the DNA/RNA-helicase Schlafen 11 (SLFN11), which has gained increasing attention since it was for the first time described as a biomarker that predicts cancer cell response to DNA damaging agents in 2012 [5].

SLFN11 binds to replication protein A (RPA) at the replication fork in response to replication stress caused by factors including cisplatin-induced DNA damage, resulting in an irreversible block of replication

Abbreviations: ATR, Ataxia telangiectasia and Rad3-related; BRCA1, Breast cancer type 1 susceptibility protein; cDDP, Cisplatin; CHK1, Checkpoint kinase 1; DNMT, DNA methyltransferase; EZH2, Enhancer of zeste homolog 2; GAPDH, Glyceraldehyde 3-phosphate dehydrogenase; HDAC, Histone deacetylase; Rad51, DNA repair protein Rad51 homolog 1; siRNA, Small interfering RNA; SLFN11, Schlafen 11; WEE1, Mitosis inhibitor protein kinase WEE1.

* Corresponding author.
E-mail address: gbendas@uni-bonn.de (G. Bendas).

https://doi.org/10.1016/j.bbadis.2024.167448
Received 23 December 2023; Received in revised form 30 July 2024; Accepted 30 July 2024
Available online 6 August 2024

and, subsequently, cell death [6]. Therefore, the expression of SLFN11 correlates with sensitivity to stress inducing agents [6]. In agreement, SLFN11 expression has been established as a clinical biomarker that predicts the response of different cancers to platinum-based chemotherapies [7–9]. Moreover, epigenetic downregulation of SLFN11 is a resistance mechanism that protects ovarian cancer cells from DNA-damaging agents including cisplatin [10]. Tumor cells can epigenetically suppress SLFN11 expression by mechanisms including histone deacetylation by HDACs [11], histone methylation by EZH2 [12], or promoter methylation by DNMTs [10]. Various epigenetic agents are under investigation that can reverse tumor suppressor downregulation and re-sensitize cancer cells to cytotoxic agents [13]. Hence, epigenetic re-induction of SLFN11 expression may have potential for this cancer entity.

Interestingly, clinical specimens of ovarian cancer patients displayed lower SLFN11 levels than other cancer entities [14,15]. This fact raises the question how DNA damages, caused by cytotoxic agents were processed downstream of SLFN11, and how resistance is caused in SLFN11 deficient cells. It has been reported that those cells rely on fork protection by Ataxia telangiectasia and Rad3 related protein (ATR) and the downstream mediated cell cycle arrest [16]. ATR kinase is a major component of the DNA damage response (DDR) pathway, which is a cellular counter reaction to genotoxic stress. It senses damaged genome and induces an arrest of the cell cycle via downstream kinases like CHK1 and WEE1 [17,18] and triggers several DNA repair pathways [19]. Small-molecule inhibitors tackling the indicated kinases involved in DDR were undergoing clinical investigation, promising a novel way to attack cancer cells and thereby reducing side effects [20–22]. However, in terms of an acquired cisplatin resistance in ovarian cancer, the knowledge on the impact of SLFN11 downregulation and activity, or the interplay of SLFN11 with the downstream DDR enzymes remains rare.

Here, we investigated whether SLFN11 expression levels correlate with cisplatin sensitivity in cisplatin-sensitive and -resistant ovarian cancer cell lines. Moreover, we examined whether epigenetic drugs can induce SLFN11 expression in SLFN11-low cells and sensitize them to cisplatin. In these terms, we uncover ATR as a more general target for combinational therapy to overcome resistance.

2. Materials and methods

2.1. Cell culture

The human ovarian cancer cell line W1 and its cisplatin-resistant subtype W1CR were a kind gift by Dr. R. Januchowski (Zielona Gora, Poland) and were first described in [23]. A2780 and cisplatin-resistant variant A2780cis, described in [24], were obtained from ECACC, UK (No. 93112519; No. 93112517-A2780cis). EFO21 and EFO27 were obtained from DSMZ (Braunschweig, Germany) and Kuramochi from JRCB (Osaka, Japan). The cisplatin-resistant Kuramochi subline Kuramochi^{r}CDDP^{2000} was derived from The Resistant Cancer Cell Line (RCCL) collection [25,26]. SKOV-3 cells were obtained from ATCC (#HTB-77). All cell lines were cultivated in RPMI 1640 medium (PAN biotech GmbH, Aidenbach, Germany) supplemented with 100 IU/mL penicillin, 100 µg/mL streptomycin and 10 % fetal calf serum (FCS) (PAN biotech GmbH) at 37 °C and 5 % CO_2. In order to maintain cisplatin resistance in W1CR, A2780cis and Kuramochi^{r}CDDP^{2000} cells, they were regularly treated with 2000 ng/mL cisplatin (Sigma-Aldrich GmbH, Steinheim, Germany). The first passage of cells following this treatment was not used for experiments to avoid adulteration by the cisplatin. The absence of mycoplasma in cell culture was confirmed every month.

2.2. Small-molecule inhibitors

For the pre-treatment in cytotoxicity assays, RT-qPCR, Western Blots, apoptosis assay, and cell cycle experiments the following inhibitors were used (see Table 1):

2.3. Cell viability assay

In order to determine the impact of cisplatin and the indicated small molecule kinase inhibitors on cell viability, MTT-assay was applied using 3-(4,5-dimethylthiazol-2-yl)-2,5-diphenyltetrazolium bromide (BioChemica, Applichem GmbH, Darmstadt, Germany). All cell lines were seeded out in triplicates in 96-well plates (Sarstedt AG & Co, Nümbrecht, Germany). W1, W1CR, A2780 and A2780cis cells were seeded at a density of 10^4 cells/well, respectively and EFO21, Kuramochi and Kuramochi^{r}CDDP^{2000} cells at a density of 5×10^3 cells/well, respectively. The next day, cells were treated with a half logarithmic dilution series of either cisplatin (10^{-4} to 10^{-8} M) or ATR inhibitor elimusertib ($10^{-4.5}$ to $10^{-8.5}$ M) and incubated for 72 h. At the end of incubation time, 20 µL of a solution of MTT (5 mg/mL) was added for 1 h at 37 °C and 5 % CO_2 in each well. After removing the supernatant, formazan crystals were solved in 200 µL DMSO per well. Finally, absorption was analyzed at 570 nm and background was subtracted at 690 nm using a plate reader (Thermomultiscan EX, Thermo, Schwerte, Germany).

For combination treatment approaches, small molecule inhibitors against ATR (elimusertib), CHK1 (SCH900776) or WEE1 (adavosertib) were used at non-toxic concentrations. The sub-toxic dose strategy is described in [27]. The cells were pre-treated with a solution of the respective inhibitor for 4 h before cisplatin was added. Dose response curves were generated by non-linear regression and a four-parameter logistic equation with variable hill slope. For calculation of IC_{50} values, the points of inflexion of the resulting sigmoidal curves were determined. Prior to statistical analysis, the values were converted in pIC_{50}. For calculation of the combination index (CI), SynergyFinder Plus was applied [28].

2.4. Treatment with epigenetically active compounds

To examine the effect of SLFN11 re-expression, cells were treated with either entinostat [1 µM] or decitabine [5 µM] or tazemetostat [10 µM] for 24 h prior to seeding in 96-well plates. To maintain epigenetically activity, entinostat at 0.1 µM, decitabine at 1 µM or tazemetostat at 5 µM, respectively was added to cellular medium in each well during seeding process.

2.5. RT-qPCR

Cells were seeded at a density of 2×10^6 cells in culture flasks and cultivated overnight at 37 °C and 5 % CO_2. The next day, they were treated with entinostat at 0.1 µM or 1 µM, decitabine at 1 µM or 5 µM or tazemetostat at 5 µM or 10 µM, respectively, and incubated for 24 h. After detaching and several washing steps with PBS, cell pellets were collected and mRNA was isolated using Direct-zol RNA Miniprep kit obtained from Zymo Research Europe GmbH (Freiburg, Germany). After mRNA quantification using Colibri Microvolume Spectrometer

Table 1
Small-molecule inhibitors used in this study.

Inhibitor	Target	Purchased from
Elimusertib (BAY1895344)	ATR	Hölzel Diagnostika Handels GmbH (Cologne, Germany)
SCH900776 (MK-8776)	CHK1	
Adavosertib (AZD1775)	WEE1	
Decitabine	DNMT	
Entinostat	HDAC class I	Biozol Diagnostica Vertrieb GmbH (Eching, Germany)
Tazemetostat	EZH2	Abcam plc (Cambridge, UK)

(Berthold Technologies, Bad Wildbad, Germany), 25 ng mRNA of each probe were used for further processing. After synthesis of cDNA (48 °C, 30 min and 95 °C, 10 min), denaturation (95 °C, 15 s), annealing and elongation (60 °C, 60 s) were performed for 45 cycles in CFX Opus 96 RT-PCR system (BioRad Laboratories GmbH, Munich, Germany). Detection of fluorescence occurred using Power SYBR Green RT-PCR Mix (Applied Biosystems, Waltham, USA). The following primer sets were used: SLFN11 (target gene) obtained from OriGene Technologies GmbH (Herford, Germany), GAPDH and β-Actin (housekeeping genes) were obtained from Biomol GmbH (Hamburg, Germany). Quantification of gene expression was performed using CFX Maestro 2.2 software (BioRad). Samples were analyzed in doublets per plate in at least 3 independent runs. The gene expression was quantified using ΔΔCq-method after normalization to housekeeping gene expression (see Table 2).

2.6. Western blot

After cell lysis and total protein quantification via Pierce™ BCA Protein Assay Kit (Thermo Fisher Scientific Inc., Waltham, USA) as described in [29], SDS-Page was performed using stain-free gels (Bio-Rad). Transfer to PVDF-membrane was made with Trans-Blot® Turbo ™ system (BioRad). After blocking using non-fat dry milk powder at a concentration of 5 % in TBS-T for 1 h, membranes were incubated with different primary-antibody solutions overnight. Mouse anti-GAPDH (#T0004; GeneTex, Irvine, USA), rabbit anti-pATR (#2853T), rabbit anti-pBRCA1 (#9009T), rabbit anti-pCHK1 (#2348T) (all purchased from Cell Signaling Technology, Frankfurt am Main, Germany), mouse anti-α-tubulin (#sc-8035), mouse anti-ATR (#sc-515173), mouse anti-BRCA1 (#sc-6954), mouse anti-CHK1 (#sc-8408), mouse anti-Rad51 (#sc-53428) and mouse anti-SLFN11 (#sc-374339) (all purchased from Santa Cruz Biotechnology, Heidelberg, Germany) diluted in TBS-T containing 1 % BSA and 0.05 % sodium azide were used. The next day, membranes were incubated with goat anti-rabbit or anti-mouse IgG kappa binding protein IgG HRP-conjugated (Santa Cruz Biotechnology) diluted in TBS-T containing 5 % non-fat dry milk powder for 2 h. The bands were visualized using Clarity Western ECL substrate chemiluminescence kit (BioRad) and ChemiDoc XRS+ imaging acquiring system (BioRad). Analysis and quantification were made in ImageLab software v 6.0 (BioRad), band intensities were normalized to total protein expression. Additionally, loading controls α-tubulin or GAPDH, respectively, were run on the same membrane as the target proteins.

2.7. Apoptosis assay

Cells were seeded at a density of 2×10^5 cells in 6-well plates (Sarstedt AG & Co) and incubated overnight at 37 °C and 5 % CO_2. The next day, cells were treated with cisplatin at 1 μM, elimusertib at 10 nM, the combination of both agents or with PBS as negative control, respectively. After 72 h, cells were detached using trypsin (PAN Biotech GmbH), washed several times with PBS and centrifugated at 450 ×*g*. The supernatant was discarded and cell pellets were solved in Annexin Binding Buffer (BioLegend Inc., San Diego, USA) containing FITC-Annexin V (BioLegend Inc.) and Propidium Iodide (PI) (Thermo Fisher Scientific Inc.) and incubated for 15 min protected from light at room temperature. Finally, cells were analyzed using Guava® easyCyte HT 11 Flow Cytometer (Luminex Corporation, Austin, TX, the USA) and FlowJo™ v10.5.3 Software (BD Life Sciences, Franklin Lakes, NJ, USA).

Table 2
Sequences of the primers used for RT-qPCR.

Target gene	Sequence (5′-3′)
SLFN11	forward: AGCCTGACAACCGAGAAATGGG reversed: GGAGTACACTGGTCTGCTAAGG
GAPDH	forward: GAGTCAACGGATTTGGTCGT reversed: TTGATTTTGGAGGGATCTCG
β-actin	forward: GGACTTCGAGCAAGAGATGG reversed: AGCACTGTGTTGGCGTACAG

2.8. Cell cycle analysis

Cells were seeded at a density of 2×10^6 cells in culture flasks and cultivated overnight at 37 °C and 5 % CO_2. The next day, cells were treated with cisplatin at 1 μM, elimusertib at 10 nM, the combination of both agents or with PBS as negative control, respectively, for 24 h. Afterwards, the assay was proceeded as described in [30]. Cell cycle was analyzed using Guava® easyCyte HT 11 Flow Cytometer (Luminex Corporation) and FlowJo™ v10.5.3 Software (BD Life Sciences).

2.9. EdU assay

Cells were seeded at a density of 4×10^5 cells in 6-well plates (Sarstedt AG & Co) and incubated overnight at 37 °C and 5 % CO_2. The next day, cells were treated with cisplatin at 1 μM, elimusertib at 10 nM, the combination of both agents or with PBS as negative control, respectively for 24 h. Then, cells were treated with EdU at 10 μM for 2 h. Afterwards, cells were detached using trypsin (PAN Biotech GmbH), fixed, permeabilized and stained with EdU using the EdU Flow Cytometry Kit (Sigma-Aldrich GmbH) according to the manufacturers instruction. Finally, cells were stained with DAPI (Cytecs, Münster, Germany) and analyzed using Guava® easyCyte HT 11 Flow Cytometer (Luminex Corporation) and FlowJo™ v10.5.3 Software (BD Life Sciences). S-phase cells were gated by single stained controls.

2.10. Knockdown of ATR via siRNA transfection

For transfection with siRNA, A2780, A2780cis, W1, and W1CR cells were seeded in 6-well plates in antibiotic-free medium at a density of 3.5×10^5 cells per well and incubated overnight at 37 °C and 5 % CO_2. The following day, cells were treated with 6 μL of ATR siRNA or control siRNA-A and transfection reagent in transfection medium (all purchased from Santa Cruz Biotechnology). Subsequently, the transfection was performed as described by the manufacturer. One day after replacement of the transfection mixture, cells were seeded for cytotoxicity assay and lysates were harvested as described previously.

2.11. Statistical analysis

The statistical analysis was performed using GraphPad Prism 8 (GraphPad Software, San Diego, CA, USA). All data are represented as mean ± SD. For comparison of two groups, unpaired *t*-test was used. For comparisons between more than two groups, one-way ANOVA following Tukey's test was performed. To check for significances between several groups and a control, one-way ANOVA following Dunnett's test was used (asterisks indicate $*p < 0.05$; $** p < 0.01$; $***p < 0.001$; $****p < 0.0001$).

3. Results

3.1. SLFN11 expression is not consistently linked to cisplatin resistance

We analyzed the ovarian cancer cell lines W1, A2780, and Kuramochi and their cisplatin-resistant sublines W1CR, A2780cis, and Kuramochi^{r}CDDP^{2000} for their resistance status and SLFN11 protein levels. The resistant sublines displayed in case of W1CR a 4.2-fold, in case of A2780cis a 5.5-fold and in case of Kuramochi^{r}CDDP^{2000} a 4.4-fold increased cisplatin IC_{50} value compared to the respective parental cell lines (Fig. 1A). We also included the ovarian cancer cell line EFO21, that displayed similar cisplatin IC_{50} values as the cisplatin-adapted cell lines, as well as sensitive EFO27 and SKOV-3 cells (Fig. 1A).

In agreement with the hypothesis that high SLFN11 levels increase

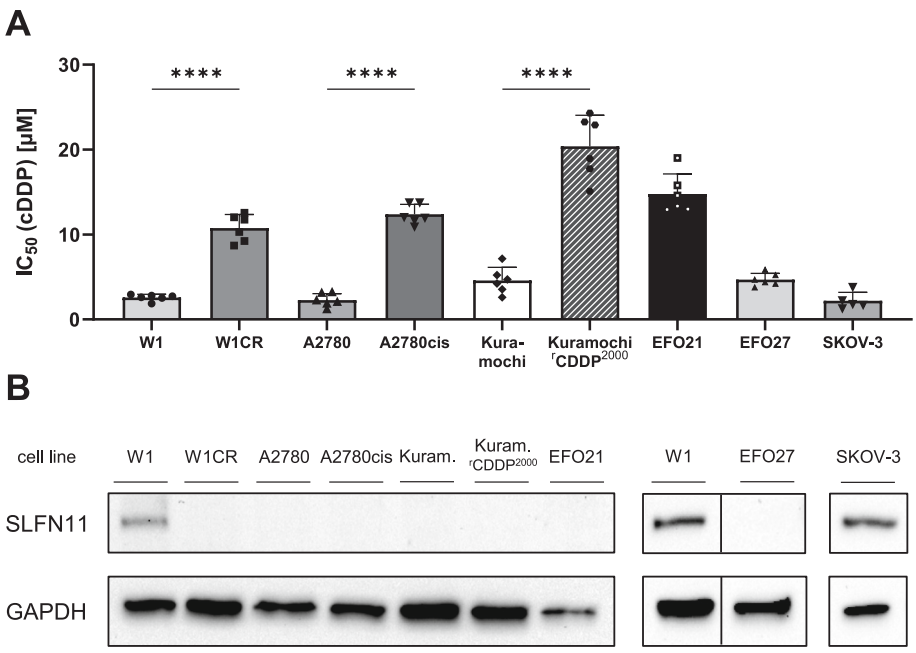

Fig. 1. **A**, IC_{50} values of cisplatin cytotoxicity in W1, A2780, Kuramochi ovarian cancer cells and their respective cisplatin-resistant subtypes W1CR, A2780cis and Kuramochi^{r}CDDP^{2000} cells, as well as in EFO21, EFO27, and SKOV-3 cells. Data refer to a four- to fix-fold higher IC_{50} values in the indicated resistant cells compared to the sensitive cells. Data represent means ± SD of at least five independent experiments. Statistical analysis was performed by unpaired *t*-tests. ****$p < 0.0001$. **B**, Expression of SLFN11 at the protein level shown as a representative example of a Western Blot in the investigated cell pairs W1/W1CR, A2780/A2780cis, Kuramochi/Kuramochi^{r}CDDP^{2000} and EFO21. W1 and EFO27 were detected on the same membrane and exposure time but bands were non-adjacent and therefore separated by a black line. SKOV-3 has been analyzed on a separate membrane with the same exposure time.

cisplatin sensitivity, SLFN11 levels were strongly reduced in cisplatin-resistant W1CR cells relative to the parental W1 cell line (Fig. 1B). However, with the exception of SKOV-3 cells, none of the other cell lines displayed significant SLFN11 levels. These data suggest that SLFN11 is not universally involved in determining cisplatin sensitivity in ovarian cancer cells.

3.2. Silencing of SLFN11 can be reversed by HDAC-inhibition antagonizing cisplatin resistance

SLFN11 is known to be epigenetically downregulated in tumor cells by various mechanisms affecting the sensitivity to DNA damage inducing agents [16]. However, the potential of epigenetic agents to re-establish SLFN11 expression and to sensitize a still existing resistance of cancer cells to DNA damage has not been explicitly studied, yet. Hence, we next investigated whether the targeting of epigenetic enzymes induces the re-expression of SLFN11 in ovarian cancer cells and affects their sensitivity to cisplatin following the approach outlined in Fig. 2A. The HDAC inhibitor entinostat (but not the DNMT inhibitor decitabine or the EZH2 inhibitor tazemetostat) increased SLFN11 in W1 and W1CR cells at the mRNA (Fig. 2B) and at the protein level (Fig. 2C) and sensitized both cell lines to cisplatin treatment (Fig. 2D). Notably, entinostat re-sensitized W1CR cells to cisplatin to the level of the parental W1 cells.

To follow a probable mode of action how entinostat antagonizes the acquired resistance in W1CR cells, an insight into DNA repair capacity was provided by Western Blot of potential associated components. Notably, entinostat at the higher concentration of 1 µM reduces the kinase CHK1 as well as BRCA1 and Rad51 in W1CR cells indicating that upregulated SLFN11 induces a downregulation of important DNA-repair proteins.

In A2780 and A2780cis cells, entinostat induced only a moderate increase of the SLFN11 mRNA levels (Fig. 3A), which is not reflected at the protein levels (Fig. 3B). Hence, the moderate sensitization of A2780 and A2780cis cells to cisplatin by entinostat (Fig. 3C) does not seem to be mediated via SLFN11 modulation. Decitabine and tazemetostat did not affect SLFN11 mRNA or protein levels in A2780 and A2780cis cell lines.

To further evaluate whether entinostat induces SLFN11 in the intrinsically resistant EFO21 cell line affecting the sensitivity to cisplatin, cells were treated with the indicated concentrations of entinostat. Using 1 µM of the HDAC inhibitor, EFO21 cells display a slight upregulation of SLFN11 (Fig. 3D) reflected by a significant decrease in the IC_{50} value (Fig. 3E).

Taken together, SLFN11 determines the cisplatin response only in a subset of ovarian cancer.

3.3. ATR is a key mediator of cisplatin resistance irrespectively of the SLFN11-phenotype

SLFN11-negative cells have been reported to depend critically on ATR signaling for mediating cell cycle arrest in response to DNA damaging agents, such as cisplatin [16]. Hence, we investigated whether the highly selective ATR-inhibitor elimusertib (BAY1895344) [31] affects the cisplatin sensitivity of W1, W1CR, A2780, and A2780cis cells.

W1CR cells displayed a reduced elimusertib sensitivity compared to W1, whereas A2780 and A2780cis cells were similar sensitive to this compound (Fig. 4A). Based on the drug response profiles, 10 nM was selected, as non-toxic concentration of elimusertib for the examination of the impact of ATR inhibition on cisplatin sensitivity in the investigated cell lines (Fig. 4A).

The presence of 10 nM elimusertib significantly decreased the cisplatin IC_{50}s of all investigated cell lines (Fig. 4B), with W1CR and A2780cis cells being sensitized to cisplatin to the level of the respective parental cell lines. The Annexin/PI assay indicated that combined elimusertib /cisplatin treatment resulted in enhanced numbers of apoptotic cells with a more pronounced combined effect observed in the cisplatin-resistant sublines (Fig. 4C, D).

In summary these data suggest a key role of ATR in mediating cisplatin resistance in ovarian cancer cells.

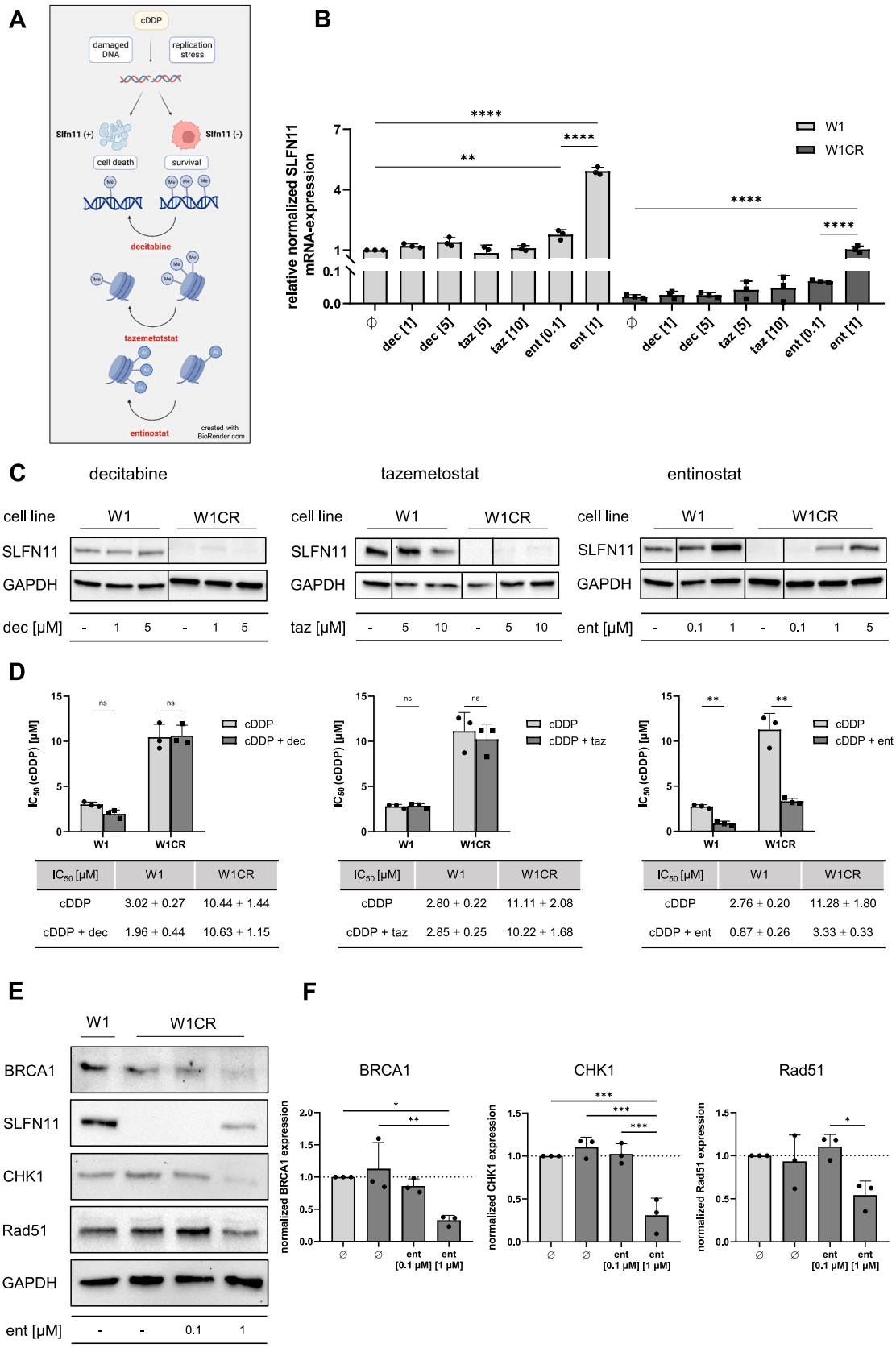

(caption on next page)

Fig. 2. Targeting of SLFN11-expression by epigenetically active drugs. **A**, Scheme illustrates the impact of SLFN11 on response to cisplatin treatment and the approach to modify its expression by the indicated epigenetic targets. **B**, Gene expression of SLFN11 under treatment with either decitabine, tazemetostat or entinostat at the indicated concentrations in μM in W1 and W1CR cells, normalized to untreated W1 cells. **C** Protein expression of SLFN11 and the respective loading control GAPDH under treatment with either decitabine, tazemetostat, or entinostat in W1 and W1CR cells. The bands of the shown Western Blots for each of the described inhibitors originate from the same membrane and exposure time, respectively. Bands that were non-adjacent and cropped together are separated by a black line. **D**, IC_{50} values of cisplatin in W1 and W1CR cells to investigate the impact of pretreatment with the indicated inhibitors on cisplatin response. Data represent means ± SD of at least three independent experiments. **E**, The impact of entinostat treatment of W1CR cells on DNA repair components indicated by representative Western Blots in an overview and **F**, quantified by normalization on untreated W1-cells, referring to a reverse relationship of SLFN11 and DNA repair capacity. Statistical analysis of multiple comparisons in **B** and **F** was performed by One-way ANOVA following Tukey's test. For the comparison of two groups (**D**), unpaired *t*-tests was used. $*p < 0.05$; $**p < 0.01$; $***p < 0.001$; $****p < 0.0001$.

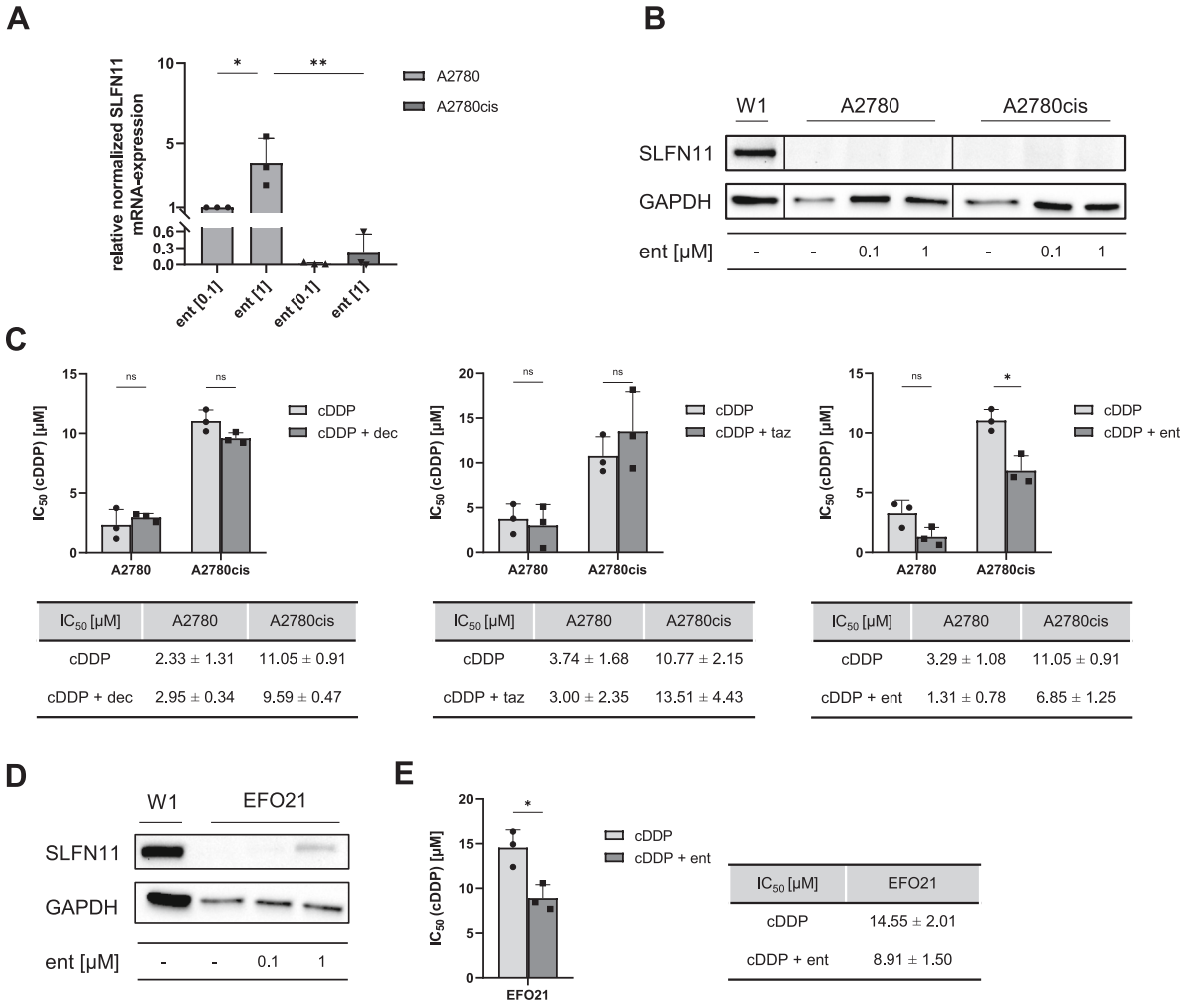

IC_{50} [μM]	A2780	A2780cis
cDDP	2.33 ± 1.31	11.05 ± 0.91
cDDP + dec	2.95 ± 0.34	9.59 ± 0.47

IC_{50} [μM]	A2780	A2780cis
cDDP	3.74 ± 1.68	10.77 ± 2.15
cDDP + taz	3.00 ± 2.35	13.51 ± 4.43

IC_{50} [μM]	A2780	A2780cis
cDDP	3.29 ± 1.08	11.05 ± 0.91
cDDP + ent	1.31 ± 0.78	6.85 ± 1.25

IC_{50} [μM]	EFO21
cDDP	14.55 ± 2.01
cDDP + ent	8.91 ± 1.50

Fig. 3. **A**, Gene expression of SLFN11 under treatment with entinostat at the indicated concentrations in μM in A2780 and A2780cis cells, normalized to A2780 cells treated with 0.1 μM entinostat. **B**, Protein expression of SLFN11 and the respective loading control GAPDH under treatment with entinostat in A2780 and A2780cis cells. Untreated W1 cells serve as positive control. The bands of the shown Western Blot originate from the same membrane and exposure time. Bands that were non-adjacent and cropped together are separated by a black line. **C**, Impact of pretreatment with the indicated inhibitors on cisplatin cytotoxicity in A2780 and A2780cis cells. **D**, Protein expression of SLFN11 and the respective loading control GAPDH under treatment with entinostat in EFO21 cells. **E**, Impact of pretreatment with entinostat on cisplatin cytotoxicity in EFO21 cells. Data represent means ± SD of at least three independent experiments. Statistical analysis of multiple comparisons in **A** was performed by One-way ANOVA following Tukey's test. For the comparison of two groups (**C**, **E**), unpaired *t*-tests was used. $*p < 0.05$; $**p < 0.01$.

Cellular levels of ATR and phosphorylated ATR were differently modulated by elimusertib and/or cisplatin treatment. In W1 and W1CR cells, 1 μM cisplatin neither affected the ATR nor the pATR levels (Fig. 5A). Elimusertib (10 nM) caused a moderate reduction of phosphorylated ATR in both cell lines, which was considerably diminished in combination with cisplatin (Fig. 5A).

In A2780 and A2780cis cell, ATR phosphorylation/activation was increased by both cisplatin (1 μM) and elimusertib (10 nM) treatment compared to the untreated controls (Fig. 5B). However, the combination of elimusertib and cisplatin also resulted in a substantial reduction of ATR activation (Fig. 5B). The investigation of CHK1 and pCHK1 levels further showed that the parental W1 and A2780 cell lines displayed a more pronounced increase of CHK1 phosphorylation/activation than their cisplatin-resistant sublines in response to cisplatin treatment (Fig. 5C, D). Elimusertib only prevented CHK1 activation in W1 and A2780 cells, but not in W1CR and A2780cis cells (Fig. 5C, D). The exact quantification of protein activation is presented by a calculated ratio in Supplement Fig. 1.

siRNA-mediated ATR depletion resulted in lower cisplatin IC_{50} values in the cisplatin-resistant sublines W1CR and A2780cis, but not in

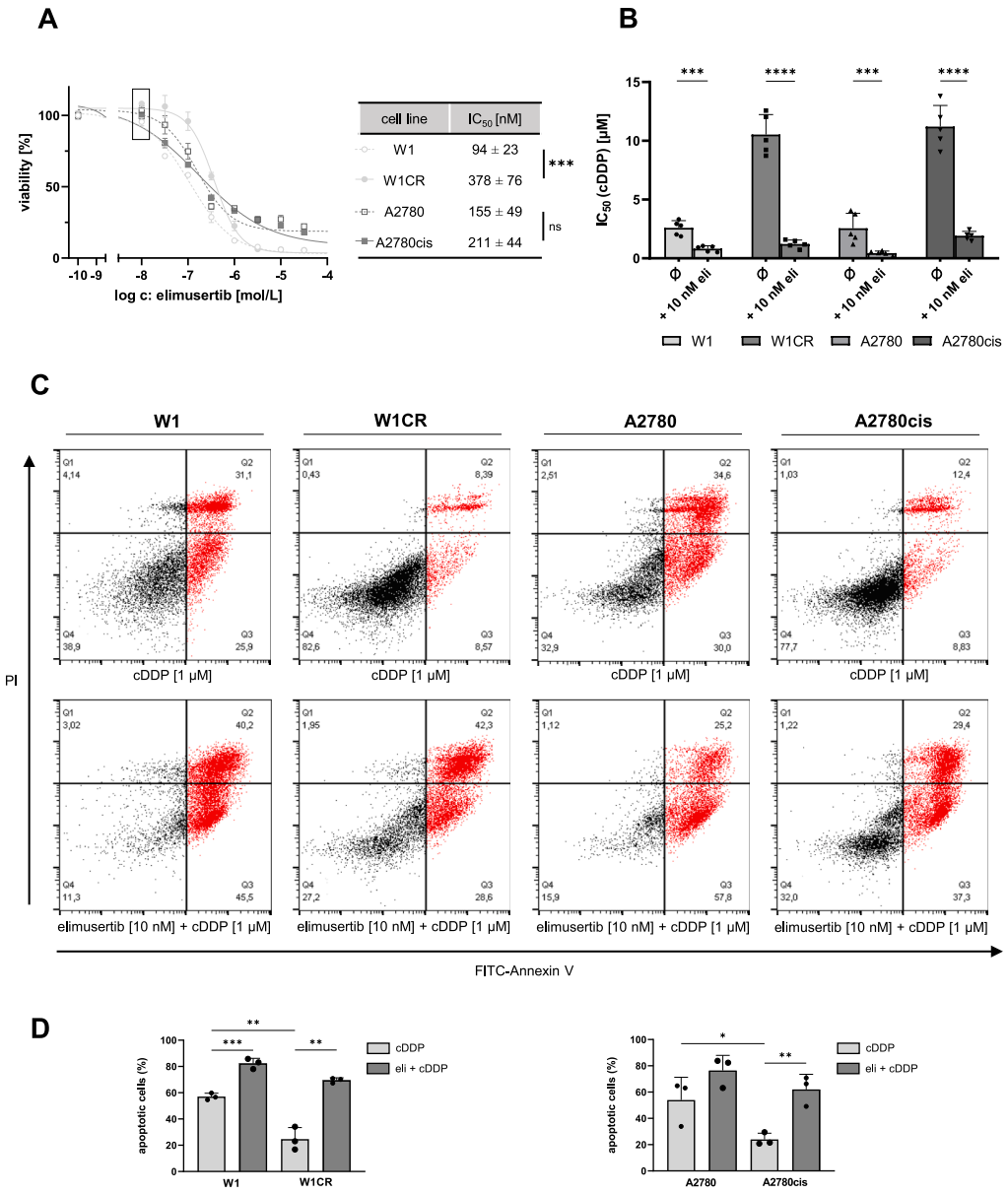

Fig. 4. Impact of selective ATR-inhibition by elimusertib on response to cisplatin. **A**, Dose-response curve of solo-treatment with elimusertib in W1, W1CR, A2780 and A2780cis cells. Rectangle indicates the concentration of elimusertib used in the following combinational treatment approaches. Table next to the curve represents the mean IC_{50} values ± SD of elimusertib. **B**, Combinational treatment of elimusertib at a sub-toxic concentration and cisplatin in W1, W1CR, A2780 and A2780cis cells. **C**, Insight into cell damage provided by representative dotplots of FITC-Annexin V/PI stained cells treated with either cisplatin or a combination of elimusertib and cisplatin. Quadrants separate populations in necrotic (Q1), late apoptotic (Q2), early apoptotic (Q3) and viable cells (Q4). **D**, Histograms show the amount of apoptotic cells at the indicated treatments. Data represent means ± SD of at least three independent experiments. Statistical analysis was performed by unpaired *t*-tests. $*p < 0.05$; $**p < 0.01$; $***p < 0.001$; $****p < 0.0001$.

the parental cell lines (Fig. 5E). The differences may be explained by the moderate depletion levels of this knockdown approach that only resulted in significant effects in the cisplatin-resistant cells, in which ATR inhibition by elimusertib had also resulted in more pronounced cisplatin sensitization. However, these data emphasize the role of ATR in the cisplatin resistance of these cells.

3.4. Complex role of ATR downstream targets in the context of cisplatin resistance

To investigate the mechanisms underlying ATR inhibition-mediated cisplatin sensitization further, we first analyzed the impact of elimusertib and cisplatin on the cell cycle of W1, W1CR, A2780, and A2780cis cells (Fig. 6A). W1CR cells, but not A2780cis cells, displayed a higher fraction of cells in S-phase than the respective parental cell line (Fig. 6A). Cisplatin and elimusertib treatment did not result in consistent cell cycle changes. Cisplatin increased the percentage of cells in S-phase in A2780 cells. Moreover, the elimusertib/cisplatin combination reduced the fraction of W1 and A2780 cells in the S-phase and induced an accumulation of A2780 cells in G2/M phase (potentially due to a defective S-phase checkpoint) (Fig. 6A). Other significant cell cycle changes were not detected by this basic assay. To further investigate the mediation of cell cycle arrest by ATR and its downstream kinases in S-phase (Fig. 6B), we performed an EdU assay to focus on proliferation of cells. Data in Fig. 6C show that the combination of ATR inhibition and cisplatin induces a significant decrease of the amount of S-phase cells in both, parental cell lines and W1CR. Furthermore, A2780cis cells are not affected to this extent by the combinational treatment, which also

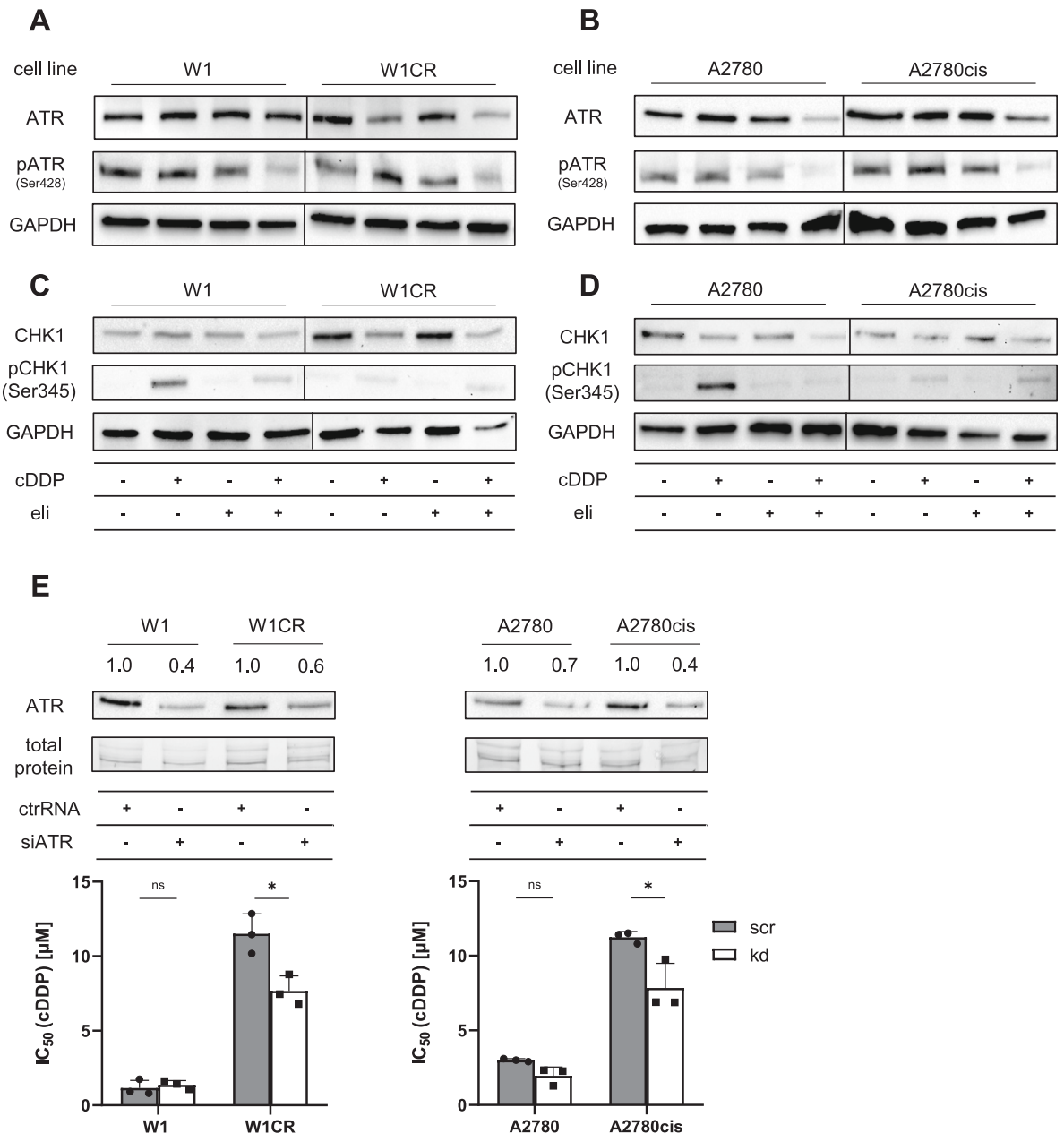

Fig. 5. Role of ATR in mediating tolerance against cytotoxic stress. **A–D**, Western Blots of ATR, pATR and the respective loading control GAPDH in W1 and W1CR cells (**A**) and A2780 and A2780cis cells (**B**) and CHK1 and pCHK1 in W1 and W1CR cells (**C**) and in A2780 and A2780cis cells (**D**) under the indicated treatments with cisplatin (cDDP) [1 µM] and elimusertib (eli) [10 nM]. The bands of the shown Western Blots in each of the subfigure (A-D) originate from the same membrane and exposure time, respectively. Bands that were non-adjacent and cropped together are separated by a black line. **E**, Western Blots of ATR and the respective loading control GAPDH in W1, W1CR, A2780 and A2780cis cells incubated with either control siRNA or ATR-knockdown siRNA. Histograms below represent IC_{50} of cisplatin in the control siRNA treated (scr) and knockdown siRNA treated cells. All data represent means ± SD of at least three independent experiments. Statistics in **A**–**D** were performed by One-way ANOVA following Tukey's test for each cell line. For comparison of change in IC_{50} values under ATR-knockdown or different treatments in **E**, unpaired *t*-tests were performed. $^{*}p < 0.05$.

approves the general cell cycle data in Fig. 6A.

Next, we investigated the impact of inhibitors of the ATR downstream targets CHK1 (SCH900776, also known as MK-8776) and WEE1 (adavosertib, also known as AZD1775) on cisplatin sensitivity, schematically shown in Fig. 6B. Non-toxic CHK1 and WEE1 inhibitor concentrations were determined (Supplement Fig. 2) and used in combination with cisplatin (Fig. 6D, E). The results revealed varying effects of non-toxic CHK1 inhibitor and WEE1 inhibitor concentrations in the two cell pairs (Fig. 6D, E), indicating differences in ATR downstream signaling between them. To further increase the informative value, the pair of Kuramochi cells and intrinsically resistant EFO21 cells were included (Fig. 6F). While ATR inhibition also sensitized these cells completely, CHK1 inhibition reversed resistance to a greater extent than blocking WEE1.

Taken together, these findings indicate that ovarian cancer cell sensitization to cisplatin by elimusertib is mediated by varying mechanisms in different cell lines. Hence, ATR inhibition is superior to the inhibition of ATR downstream targets in sensitizing ovarian cancer cells to cisplatin. Notably, the combination of elimusertib and cisplatin displayed high synergy, indicated by predominantly low to very low combinational activity scores (Supplement Fig. 3).

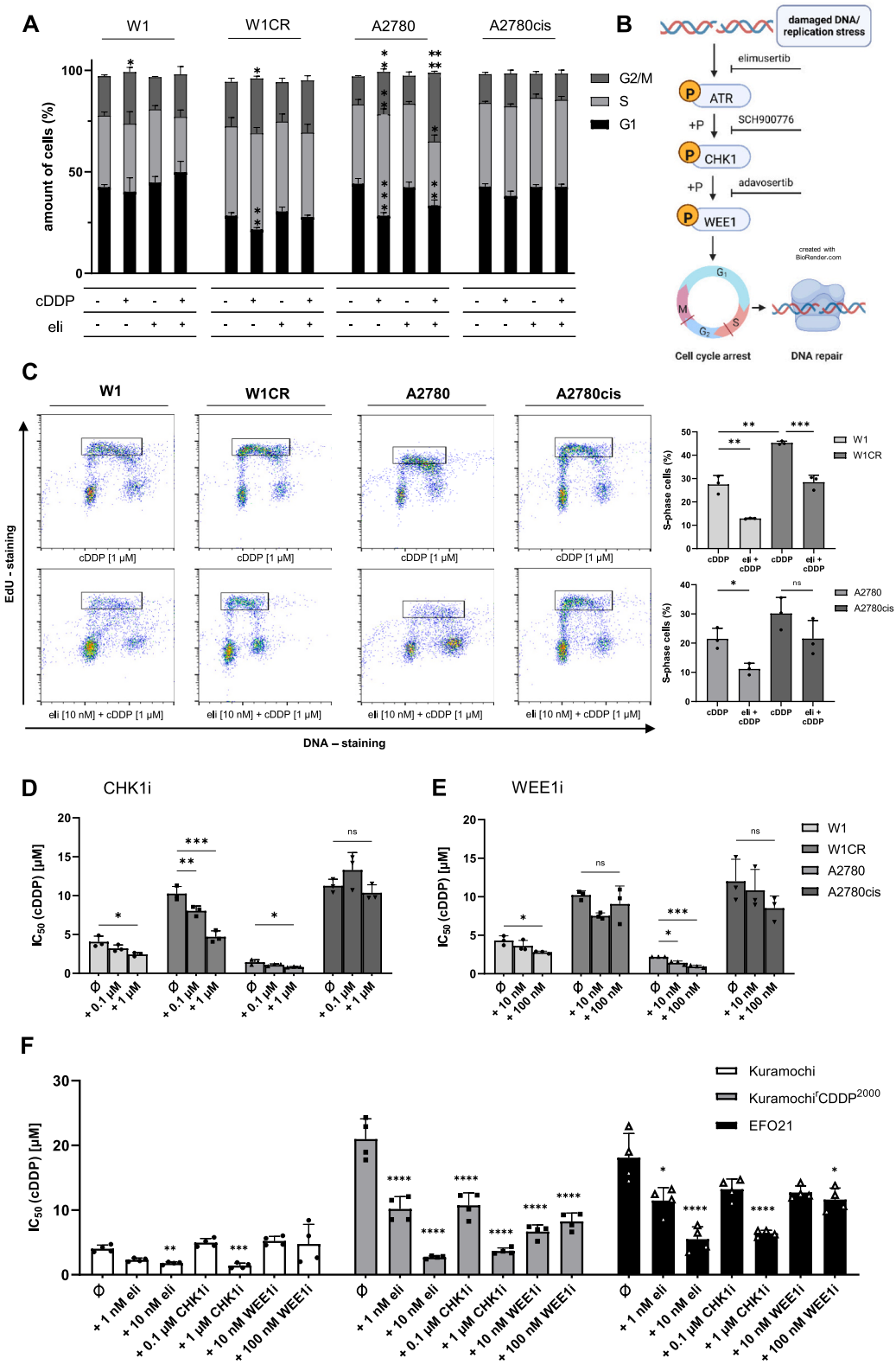

Fig. 6. Downstream signaling of ATR including cell cycle regulation and DNA damage response pathway inhibition. **A**, Cell cycle regulation upon treatment with either cisplatin, elimusertib or the combination of both. **B**, Scheme for the regulation of DNA damage response pathway and targets of the selective kinase inhibitors used in this study. **C**, Detailed insight into cell cycle regulation by representative dotplots of EdU-staining versus DNA-staining in W1, W1CR, A2780 and A2780cis cells upon treatment with cisplatin or the combination of cisplatin and elimusertib. The black rectangle indicates the population of S-phase cells that were gated by single EdU-staining. Histograms next to dotplots show the amount of S-phase cells (%) ± SD in three independent experiments. **D**, **E**, Combinational treatments of either SCH900776 (**D**) or adavosertib (**E**) at the indicated sub-toxic concentrations with cisplatin in W1, W1CR, A2780 and A2780cis cells. **F**, Combinational treatments of either elimusertib, SCH900776 or adavosertib with cisplatin at the indicated sub-toxic concentrations in Kuramochi, Kurampchi^{r}CDDP^{2000} and EFO21 cells. All data represent means ± SD of at least three independent experiments. Statistics in **A**, **D**, **E** and **F** were performed by One-way ANOVA following Dunnett's test for each cell line. Statistics in **C** were performed by unpaired *t*-test. $^{*}p < 0.05$; $^{**}p < 0.01$; $^{***}p < 0.001$; $^{****}p < 0.0001$.

3.5. Elimusertib inhibits BRCA1 activation

Since inhibition of the ATR downstream targets CHK1 and WEE1 did not result in the same cisplatin sensitization patterns as ATR inhibition, ovarian cancer cell sensitization to cisplatin by elimusertib may involve additional signaling pathways. Notably, ATR has also been reported to activate directly DNA repair via homologous recombination (HR) [19]. Hence, we next investigated the effect of elimusertib on cisplatin-

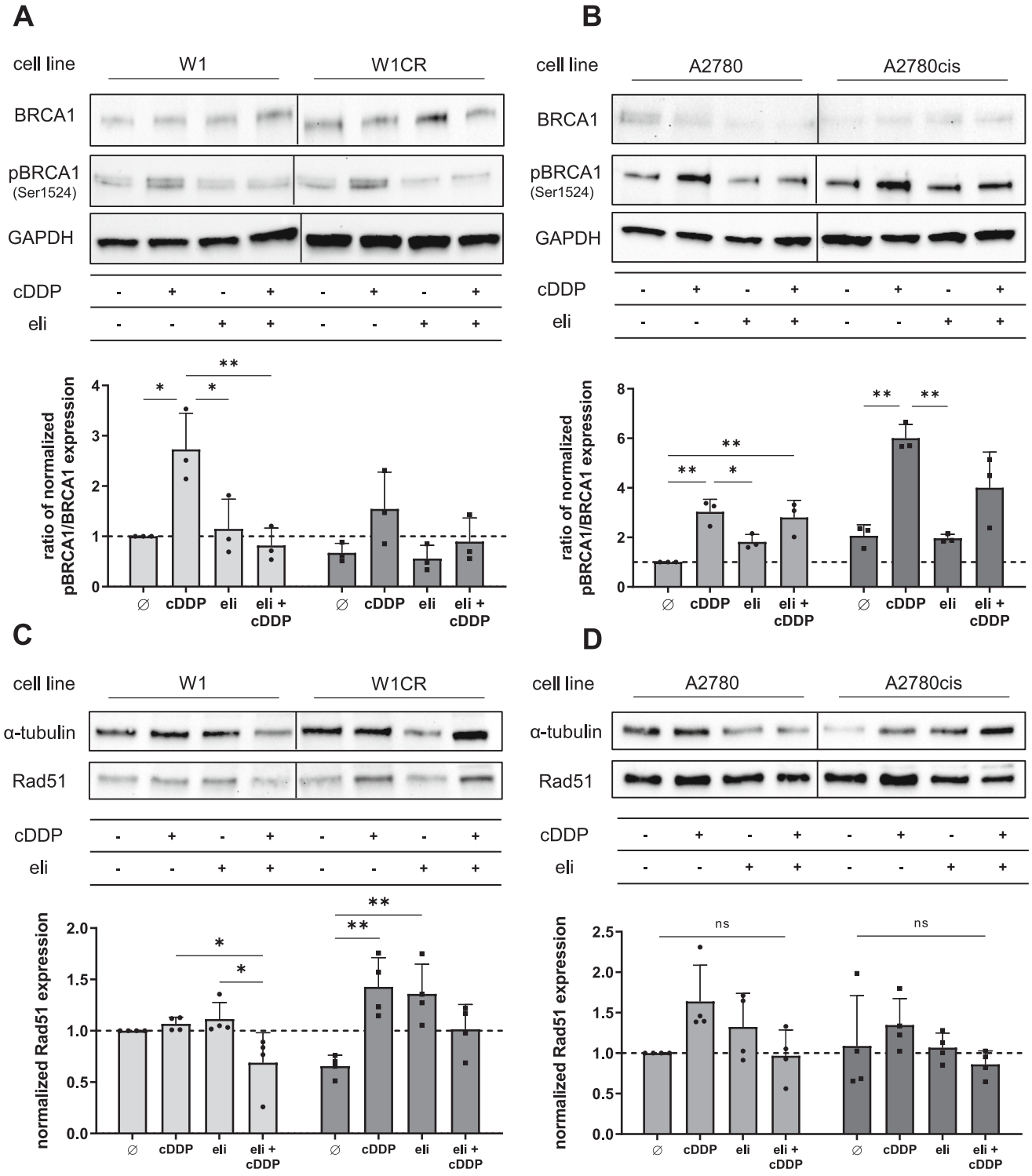

Fig. 7. Impact of ATR-inhibition on homologous combination repair. **A**, **B**, Western Blots of BRCA1 and pBRCA1 and the respective loading control GAPDH in W1 and W1CR cells (**A**) and A2780 and A2780cis cells (**B**) under the indicated treatments. Histogram below Western Blots illustrates the ratio of phosphorylated and total BRCA1-expression. Western Blots of Rad51 and the respective loading control α-tubulin in W1 and W1CR cells (**C**) and A2780 and A2780cis cells (**D**) under the indicated treatments, and normalized expression data in the histograms below. The bands of the shown Western Blots in each of the subfigure (A–D) originate from the same membrane and exposure time, respectively. Bands that were non-adjacent and cropped together are separated by a black line. All data represent means ± SD of calculated ratios in three independent experiments. Statistical analysis was performed by One-way ANOVA following Tukey's test for each cell line. $*p < 0.05$; $**p < 0.01$.

induced BRCA1 phosphorylation, which is a critical event during homologous recombination. We focused on W1 and A2780 cells and their cisplatin-resistant sublines, as the most pronounced differences regarding ATR inhibition vs. CHK1 and/or WEE1 inhibition were observed in these cell lines.

Cisplatin caused BRCA1 phosphorylation/activation in all four cell lines, which was suppressed by the ATR inhibitor elimusertib (Fig. 7A and B). Notably, elimusertib also inhibited the cisplatin-induced upregulation of Rad51, another key player in homologous recombination [32] in W1, W1CR, A2780, and A2780cis cells (Fig. 7C and D). The exact protein quantification of activated pBRCA1 and total BRCA1 is shown in Supplementary Fig. 4.

4. Discussion

Treatment of ovarian cancer fails in approx. 50 % of cases within five years due to development of chemoresistance [2]. Accordingly, novel biomarkers and therapeutic targets are needed for the treatment of therapy-refractory ovarian cancer. Absence of SLFN11-expression has gained attention as an indicator for resistance against DNA damaging agents in several cancer entities in recent years [16]. However, the potential role of SLFN11 in acquired resistance is not well understood and requires further investigation.

Here, we investigated the potential role of SLFN11 in cisplatin resistance in a panel of ovarian cancer cell lines and found that SLFN11 levels do not generally correlate with the response to cisplatin. Nevertheless, SLFN11 was shown to be involved in cisplatin resistances in individual cases. While the ovarian cancer cell line W1 displayed substantial SLFN11 protein levels, its cisplatin-resistant subline W1CR did not have detectable SLFN11 levels. W1CR treatment with the HDAC class I inhibitor entinostat re-instated SLFN11 expression and sensitized W1CR to cisplatin to the level of the parental cell line. These effects were mediated by a downregulation of DNA repair capacity which is an additive effect of entinostat and an inhibition of HR by SLFN11 which has been showed by Mu et al. [33]. Nevertheless, the expression levels of SLFN11 within cisplatin-sensitive and -resistant cells do not provide a generally valid picture, so that further research will be needed to establish an understanding of which individual cancers will benefit from SLFN11 reactivation.

SLFN11 is activated in response to DNA damage and replication stress in close proximity to, but independently of ATR-kinase [34]. SLFN11-deficient cells from several cancer entities have been reported to rely on checkpoint activation and initiation of DNA repair pathways by the ATR-CHK1 axis [35]. Hence, we next investigated the effects of the ATR inhibitor elimusertib in our ovarian cancer cell line panel. Remarkably, elimusertib sensitized all investigated cell lines to cisplatin, independently of the SLFN11 status, thereby overcoming acquired (A2780cis, Kuramochi^{r}CDDP^{2000}, W1CR cells) and intrinsic (EFO21) resistance.

The combination of elimusertib and cisplatin resulted in synergistic effects. Elimusertib inhibited cisplatin-induced ATR activation, and siRNA-mediated ATR depletion increased cisplatin activity, confirming that the elimusertib sensitization is the consequence of ATR inhibition. Interestingly, different ATR downstream signaling pathways and cell cycle regulation appear to be relevant in the context of cisplatin resistance in different cell lines. In some ovarian cancer cell lines, inhibition of the ATR downstream targets CHK1 and/or WEE1 was sufficient to reproduce the ATR inhibition-associated effects. In other cell lines, ATR inhibition by elimusertib also inhibited homologous recombination as indicated by reduced BRCA1 and Rad51 activation.

Notably, ATR inhibition has been reported to be particularly effective against p53-deficient cells [36]. Loss of *TP53* mutations has been described in >96 % of cases of high-grade serous ovarian cancer cases, the most common histological subtype [37]. In agreement, the ATR inhibitor elimusertib effectively re-sensitized the *TP53*-mutant Kuramochi cell line and its cisplatin-resistant subline to cisplatin in this study [38,39]. Kuramochi is arguably one of the commercially available cell lines that most closely reflect the mutation profile of serous ovarian cancer patient tumors [40].

In conclusion, our data provide novel insights into the roles of SLFN11 and ATR in ovarian cancer cell response to cisplatin and in a still existing cisplatin resistance of ovarian cancer cells. Although the data confirm that epigenetic SLFN11 silencing can mediate acquired cisplatin resistance in ovarian cancer, which can be overcome using HDAC inhibitors, this line of evidence is restricted by the limited number of cell lines and HDAC inhibitors used. However, these initial findings of epigenetic targeting of SLFN11 in an ovarian cancer resistance context warrants further investigations. Furthermore, continued research is needed to find biomarkers that identify patients who will benefit from such therapies. Proteins identified here that were inversely correlated with SLFN11 expression appear as potential candidates. However, it should be considered that epigenetic side-effects of entinostat are manifold and vary between the cell lines.

In contrast to SLFN11, ATR appears to sensitize a broader range of ovarian cancer cell lines to cisplatin, including drug-adapted resistant ones. Our data further show that ATR mediates cisplatin resistance by multiple pathways including activation of its downstream kinases like CHK1 and WEE1 [17,18] and of homologous recombination [19], whose importance differs between ovarian cancer cell lines. Hence, ATR inhibitors, still started to be applied in clinical trials [41], have a greater potential for broad spectrum application in the clinics than inhibitors of its downstream kinases CHK1 and WEE1 and are promising agents for overcoming cisplatin resistance in ovarian cancer. The ongoing clinical trials to sensitize patients to therapy with DNA damaging agents will also help to increase the understanding of overcoming chemoresistance.

CRediT authorship contribution statement

Philipp König: Writing – original draft, Validation, Methodology, Investigation, Formal analysis, Data curation, Conceptualization. **Julia Maria Eichhorn:** Visualization, Validation, Investigation, Formal analysis, Data curation. **Eloy Suparman:** Investigation, Data curation. **Nico Bückreiß:** Visualization, Investigation, Formal analysis, Data curation. **Jindrich Cinatl:** Writing – review & editing, Resources. **Martin Michaelis:** Writing – review & editing, Resources, Methodology. **Gerd Bendas:** Writing – original draft, Supervision, Resources, Project administration, Conceptualization.

Declaration of competing interest

The authors declare that they have no competing interest.

Data availability

Data will be made available on request.

Acknowledgments

The authors would like to thank Radoslaw Januchowski, Univ. of Zielona Gora, Poland for providing W1 and W1CR cells. Additionally, we are grateful for Florian Rothweiler who organized shipping of Kuramochi, Kuramochi^{r}CDDP^{2000} and EFO21 cells. Finally, we thank Svenja Henze and Ramona Menden who supported this project by performing Western Blots and RT-qPCR, respectively.

Appendix A. Supplementary data

Supplementary data to this article can be found online at https://doi.org/10.1016/j.bbadis.2024.167448.

References

[1] K.C. Kurnit, G.F. Fleming, E. Lengyel, Updates and new options in advanced epithelial ovarian cancer treatment, Obstet. Gynecol. 137 (2021) 108–121, https://doi.org/10.1097/AOG.0000000000004173.

[2] R.L. Siegel, K.D. Miller, N.S. Wagle, A. Jemal, Cancer statistics, 2023, CA Cancer J. Clin. 73 (2023) 17–48, https://doi.org/10.3322/caac.21763.

[3] S. Sambasivan, Epithelial ovarian cancer: review article, Cancer Treat. Res. Commun. 33 (2022) 100629, https://doi.org/10.1016/j.ctarc.2022.100629.

[4] L. Norouzi-Barough, M.R. Sarookhani, M. Sharifi, S. Moghbelinejad, S. Jangjoo, R. Salehi, Molecular mechanisms of drug resistance in ovarian cancer, J. Cell. Physiol. 233 (2018) 4546–4562, https://doi.org/10.1002/jcp.26289.

[5] G. Zoppoli, M. Regairaz, E. Leo, W.C. Reinhold, S. Varma, A. Ballestrero, J. H. Doroshow, Y. Pommier, Putative DNA/RNA helicase Schlafen-11 (SLFN11) sensitizes cancer cells to DNA-damaging agents, Proc. Natl. Acad. Sci. U. S. A. 109 (2012) 15030–15035, https://doi.org/10.1073/pnas.1205943109.

[6] J. Murai, A. Thomas, M. Miettinen, Y. Pommier, Schlafen 11 (SLFN11), a restriction factor for replicative stress induced by DNA-targeting anti-cancer therapies, Pharmacol. Ther. 201 (2019) 94–102, https://doi.org/10.1016/j.pharmthera.2019.05.009.

[7] D. Taniyama, N. Sakamoto, T. Takashima, M. Takeda, Q.T. Pham, S. Ukai, R. Maruyama, K. Harada, T. Babasaki, Y. Sekino, T. Hayashi, K. Sentani, Y. Pommier, J. Murai, W. Yasui, Prognostic impact of Schlafen 11 in bladder cancer patients treated with platinum-based chemotherapy, Cancer Sci. 113 (2022) 784–795, https://doi.org/10.1111/cas.15207.

[8] T. Takashima, D. Taniyama, N. Sakamoto, M. Yasumoto, R. Asai, T. Hattori, R. Honma, P.Q. Thang, S. Ukai, R. Maruyama, K. Harada, K. Kuraoka, K. Tanabe, A. T. Sasaki, H. Ohdan, E. Morii, J. Murai, W. Yasui, Schlafen 11 predicts response to platinum-based chemotherapy in gastric cancers, Br. J. Cancer 125 (2021) 65–77, https://doi.org/10.1038/s41416-021-01364-3.

[9] T. He, M. Zhang, R. Zheng, S. Zheng, E. Linghu, J.G. Herman, M. Guo, Methylation of SLFN11 is a marker of poor prognosis and cisplatin resistance in colorectal cancer, Epigenomics 9 (2017) 849–862, https://doi.org/10.2217/epi-2017-0019.

[10] V. Nogales, W.C. Reinhold, S. Varma, A. Martinez-Cardus, C. Moutinho, S. Moran, H. Heyn, A. Sebio, A. Barnadas, Y. Pommier, M. Esteller, Epigenetic inactivation of the putative DNA/RNA helicase SLFN11 in human cancer confers resistance to platinum drugs, Oncotarget 7 (2016) 3084–3097, https://doi.org/10.18632/oncotarget.6413.

[11] S.-W. Tang, A. Thomas, J. Murai, J.B. Trepel, S.E. Bates, V.N. Rajapakse, Y. Pommier, Overcoming resistance to DNA-targeted agents by epigenetic activation of Schlafen 11 (SLFN11) expression with class I histone deacetylase inhibitors, clinical cancer research an official journal of the American association for, Cancer Res. 24 (2018) 1944–1953, https://doi.org/10.1158/1078-0432.CCR-17-0443.

[12] E.E. Gardner, B.H. Lok, V.E. Schneeberger, P. Desmeules, L.A. Miles, P.K. Arnold, A. Ni, I. Khodos, E. de Stanchina, T. Nguyen, J. Sage, J.E. Campbell, S. Ribich, N. Rekhtman, A. Dowlati, P.P. Massion, C.M. Rudin, J.T. Poirier, Chemosensitive relapse in small cell lung cancer proceeds through an EZH2-SLFN11 axis, Cancer Cell 31 (2017) 286–299, https://doi.org/10.1016/j.ccell.2017.01.006.

[13] N. Wang, T. Ma, B. Yu, Targeting epigenetic regulators to overcome drug resistance in cancers, Sig. Transduct. Target Ther. 8 (2023) 69, https://doi.org/10.1038/s41392-023-01341-7.

[14] J. Barretina, G. Caponigro, N. Stransky, K. Venkatesan, A.A. Margolin, S. Kim, C. J. Wilson, J. Lehár, G.V. Kryukov, D. Sonkin, A. Reddy, M. Liu, L. Murray, M. F. Berger, J.E. Monahan, P. Morais, J. Meltzer, A. Korejwa, J. Jané-Valbuena, F. A. Mapa, J. Thibault, E. Bric-Furlong, P. Raman, A. Shipway, I.H. Engels, J. Cheng, G.K. Yu, J. Yu, P. Aspesi, M. de Silva, K. Jagtap, M.D. Jones, L. Wang, C. Hatton, E. Palescandolo, S. Gupta, S. Mahan, C. Sougnez, R.C. Onofrio, T. Liefeld, L. MacConaill, W. Winckler, M. Reich, N. Li, J.P. Mesirov, S.B. Gabriel, G. Getz, K. Ardlie, V. Chan, V.E. Myer, B.L. Weber, J. Porter, M. Warmuth, P. Finan, J. L. Harris, M. Meyerson, T.R. Golub, M.P. Morrissey, W.R. Sellers, R. Schlegel, L. A. Garraway, The cancer cell line encyclopedia enables predictive modelling of anticancer drug sensitivity, Nature 483 (2012) 603–607, https://doi.org/10.1038/nature11003.

[15] S.E. Willis, C. Winkler, M.P. Roudier, T. Baird, P. Marco-Casanova, E.V. Jones, P. Rowe, J. Rodriguez-Canales, H.K. Angell, F.S.L. Ng, P.M. Waring, D. Hodgson, J. A. Ledermann, J.I. Weberpals, E. Dean, E.A. Harrington, J.C. Barrett, A.J. Pierce, E. Leo, G.N. Jones, Retrospective analysis of Schlafen11 (SLFN11) to predict the outcomes to therapies affecting the DNA damage response, Br. J. Cancer 125 (2021) 1666–1676, https://doi.org/10.1038/s41416-021-01560-1.

[16] C. Winkler, J. Armenia, G.N. Jones, L. Tobalina, M.J. Sale, T. Petreus, T. Baird, V. Serra, A.T. Wang, A. Lau, M.J. Garnett, P. Jaaks, E.A. Coker, A.J. Pierce, M. J. O'Connor, E. Leo, SLFN11 informs on standard of care and novel treatments in a wide range of cancer models, Br. J. Cancer 124 (2021) 951–962, https://doi.org/10.1038/s41416-020-01199-4.

[17] D. Woods, J.J. Turchi, Chemotherapy induced DNA damage response: convergence of drugs and pathways, Cancer Biol. Ther. 14 (2013) 379–389, https://doi.org/10.4161/cbt.23761.

[18] V.A.J. Smits, D.A. Gillespie, DNA damage control: regulation and functions of checkpoint kinase 1, FEBS J. 282 (2015) 3681–3692, https://doi.org/10.1111/febs.13387.

[19] R. Buisson, J. Niraj, A. Rodrigue, C.K. Ho, J. Kreuzer, T.K. Foo, E.J.-L. Hardy, G. Dellaire, W. Haas, B. Xia, J.-Y. Masson, L. Zou, Coupling of homologous recombination and the checkpoint by ATR, Mol. Cell 65 (2017) 336–346, https://doi.org/10.1016/j.molcel.2016.12.007.

[20] Z. Qiu, N.L. Oleinick, J. Zhang, ATR/CHK1 inhibitors and cancer therapy, Radiother. Oncol. 126 (2018) 450–464, https://doi.org/10.1016/j.radonc.2017.09.043.

[21] J.A. Webster, R. Tibes, L. Morris, A.L. Blackford, M. Litzow, M. Patnaik, G. L. Rosner, I. Gojo, R. Kinders, L. Wang, L.A. Doyle, C.J. Huntoon, L.M. Karnitz, S. H. Kaufmann, J.E. Karp, B.D. Smith, Randomized phase II trial of cytosine arabinoside with and without the CHK1 inhibitor MK-8776 in relapsed and refractory acute myeloid leukemia, Leuk. Res. 61 (2017) 108–116, https://doi.org/10.1016/j.leukres.2017.09.005.

[22] S. Leijen, R.M.J.M. van Geel, A.C. Pavlick, R. Tibes, L. Rosen, A.R.A. Razak, R. Lam, T. Demuth, S. Rose, M.A. Lee, T. Freshwater, S. Shumway, L.W. Liang, A.M. Oza, J. H.M. Schellens, G.I. Shapiro, Phase I study evaluating WEE1 inhibitor AZD1775 as monotherapy and in combination with gemcitabine, cisplatin, or carboplatin in patients with advanced solid tumors, journal of clinical oncology official journal of the American society of, Clin. Oncol. 34 (2016) 4371–4380, https://doi.org/10.1200/JCO.2016.67.5991.

[23] R. Januchowski, P. Zawierucha, M. Andrzejewska, M. Ruciński, M. Zabel, Microarray-based detection and expression analysis of ABC and SLC transporters in drug-resistant ovarian cancer cell lines, Biomed. Pharmacother. 67 (2013) 240–245, https://doi.org/10.1016/j.biopha.2012.11.011.

[24] B.C. Behrens, T.C. Hamilton, H. Masuda, K.R. Grotzinger, J. Whang-Peng, K. G. Louie, T. Knutsen, W.M. McKoy, R.C. Young, R.F. Ozols, Characterization of a cis-diamminedichloroplatinum(II)-resistant human ovarian cancer cell line and its use in evaluation of platinum analogues, Cancer Res. 47 (1987) 414–418.

[25] M. Michaelis, M.N. Wass, J. Cinatl, Drug-adapted cancer cell lines as preclinical models of acquired resistance, Cancer Drug Resist. 2 (2019) 447–456, https://doi.org/10.20517/cdr.2019.005.

[26] Industrial Biotechnology Centre, The Resistant Cancer Cell Line (RCCL) Collection - Industrial Biotechnology Centre - Research at Kent. https://research.kent.ac.uk/industrial-biotechnology-centre/the-resistant-cancer-cell-line-rccl-collection/, 2023. (Accessed 20 December 2023).

[27] A. Golder, L. Nelson, A. Tighe, B. Barnes, C. Coulson-Gilmer, R.D. Morgan, J. C. McGrail, S.S. Taylor, Multiple-low-dose therapy: effective killing of high-grade serous ovarian cancer cells with ATR and CHK1 inhibitors, NAR, Cancer 4 (2022) zcac036, https://doi.org/10.1093/narcan/zcac036.

[28] S. Zheng, W. Wang, J. Aldahdooh, A. Malyutina, T. Shadbahr, Z. Tanoli, A. Pessia, J. Tang, SynergyFinder plus: toward better interpretation and annotation of drug combination screening datasets, Genomics Proteomics Bioinformatics 20 (2022) 587–596, https://doi.org/10.1016/j.gpb.2022.01.004.

[29] K. Wantoch von Rekowski, P. König, S. Henze, M. Schlesinger, P. Zawierucha, R. Januchowski, G. Bendas, The impact of integrin-mediated matrix adhesion on cisplatin resistance of W1 ovarian cancer cells, Biomolecules 9 (2019) 788, https://doi.org/10.3390/biom9120788.

[30] P. König, R. Zhulenko, E. Suparman, H. Hoffmeister, N. Bückreiß, I. Ott, G. Bendas, A biscarbene gold(I)-NHC-complex overcomes cisplatin-resistance in A2780 and W1 ovarian cancer cells highlighting pERK as regulator of apoptosis, Cancer Chemother. Pharmacol. 92 (2023) 57–69, https://doi.org/10.1007/s00280-023-04548-1.

[31] U. Lücking, L. Wortmann, A.M. Wengner, J. Lefranc, P. Lienau, H. Briem, G. Siemeister, U. Bömer, K. Denner, M. Schäfer, M. Koppitz, K. Eis, F. Bartels, B. Bader, W. Bone, D. Moosmayer, S.J. Holton, U. Eberspächer, J. Grudzinska-Goebel, C. Schatz, G. Deeg, D. Mumberg, F. von Nussbaum, Damage incorporated: discovery of the potent, highly selective, orally available ATR inhibitor BAY 1895344 with favorable pharmacokinetic properties and promising efficacy in monotherapy and in combination treatments in preclinical tumor models, J. Med. Chem. 63 (2020) 7293–7325, https://doi.org/10.1021/acs.jmedchem.0c00369.

[32] W. Zhao, J.B. Steinfeld, F. Liang, X. Chen, D.G. Maranon, C. Jian Ma, Y. Kwon, T. Rao, W. Wang, C. Sheng, X. Song, Y. Deng, J. Jimenez-Sainz, L. Lu, R.B. Jensen, Y. Xiong, G.M. Kupfer, C. Wiese, E.C. Greene, P. Sung, BRCA1-BARD1 promotes RAD51-mediated homologous DNA pairing, Nature 550 (2017) 360–365, https://doi.org/10.1038/nature24060.

[33] Y. Mu, J. Lou, M. Srivastava, B. Zhao, X. Feng, T. Liu, J. Chen, J. Huang, SLFN11 inhibits checkpoint maintenance and homologous recombination repair, EMBO Rep. 17 (2016) 94–109, https://doi.org/10.15252/embr.201540964.

[34] J. Murai, S.-W. Tang, E. Leo, S.A. Baechler, C.E. Redon, H. Zhang, M. Al Abo, V. N. Rajapakse, E. Nakamura, L.M.M. Jenkins, M.I. Aladjem, Y. Pommier, SLFN11 blocks stressed replication forks independently of ATR, Mol. Cell 69 (2018) 371–384.e6, https://doi.org/10.1016/j.molcel.2018.01.012.

[35] U. Jo, Y. Murai, S. Chakka, L. Chen, K. Cheng, J. Murai, L.K. Saha, L.M. Miller Jenkins, Y. Pommier, SLFN11 promotes CDT1 degradation by CUL4 in response to replicative DNA damage, while its absence leads to synthetic lethality with ATR/CHK1 inhibitors, Proc. Natl. Acad. Sci. U. S. A. 118 (2021) e2015654118, https://doi.org/10.1073/pnas.2015654118.

[36] L.I. Toledo, M. Murga, R. Zur, R. Soria, A. Rodriguez, S. Martinez, J. Oyarzabal, J. Pastor, J.R. Bischoff, O. Fernandez-Capetillo, A cell-based screen identifies ATR inhibitors with synthetic lethal properties for cancer-associated mutations, Nat. Struct. Mol. Biol. 18 (2011) 721–727, https://doi.org/10.1038/nsmb.2076.

[37] Integrated genomic analyses of ovarian carcinoma, Nature 474 (2011) 609–615, https://doi.org/10.1038/nature10166.

[38] B.M. Barnes, L. Nelson, A. Tighe, G.J. Burghel, I.-H. Lin, S. Desai, J.C. McGrail, R. D. Morgan, S.S. Taylor, Distinct transcriptional programs stratify ovarian cancer cell lines into the five major histological subtypes, Genome Med. 13 (2021) 140, https://doi.org/10.1186/s13073-021-00952-5.

[39] Y. Yaginuma, H. Westphal, Abnormal structure and expression of the p53 gene in human ovarian carcinoma cell lines, Cancer Res. 52 (1992) 4196–4199.
[40] S. Domcke, R. Sinha, D.A. Levine, C. Sander, N. Schultz, Evaluating cell lines as tumour models by comparison of genomic profiles, Nat. Commun. 4 (2013) 2126, https://doi.org/10.1038/ncomms3126.
[41] F.M. Barnieh, P.M. Loadman, R.A. Falconer, Progress towards a clinically-successful ATR inhibitor for cancer therapy, Curr. Res. Pharmacol. Drug Discov. 2 (2021) 100017, https://doi.org/10.1016/j.crphar.2021.100017.